ResearchGate

See discussions, stats, and author profiles for this publication at: https://www.researchgate.net/publication/24024068

Structures and Properties of Electronically Excited Chromophores in Solution from the Polarizable Continuum Model Coupled to the Time-Dependent Density Functional Theory

ARTICLE *in* THE JOURNAL OF PHYSICAL CHEMISTRY A · MARCH 2009

Impact Factor: 2.69 · DOI: 10.1021/jp8094853 · Source: PubMed

CITATIONS
87

READS
102

5 AUTHORS, INCLUDING:

Benedetta Mennucci
Università di Pisa
249 PUBLICATIONS **24,236** CITATIONS
SEE PROFILE

Chiara Cappelli
Scuola Normale Superiore di Pisa
117 PUBLICATIONS **1,863** CITATIONS
SEE PROFILE

Roberto Cammi
Università degli studi di Parma
152 PUBLICATIONS **16,223** CITATIONS
SEE PROFILE

Jacopo Tomasi
Università di Pisa
347 PUBLICATIONS **40,294** CITATIONS
SEE PROFILE

Available from: Ciro Achille Guido
Retrieved on: 26 January 2016

FEATURE ARTICLE

Structures and Properties of Electronically Excited Chromophores in Solution from the Polarizable Continuum Model Coupled to the Time-Dependent Density Functional Theory

Benedetta Mennucci,*,† Chiara Cappelli,† Ciro Achille Guido,‡ Roberto Cammi,§ and Jacopo Tomasi†

Dipartimento di Chimica e Chimica Industriale, Università di Pisa, Via Risorgimento 35, 56126 Pisa, Italy, Scuola Normale Superiore, Piazza dei Cavalieri 7, 56126 Pisa, Italy, and Dipartimento di Chimica, Università di Parma, Viale delle Scienze 17/A, 43100 Parma, Italy

Received: October 27, 2008; Revised Manuscript Received: January 12, 2009

Downloaded by INIST TITAN SCIENCES on September 14, 2009 | http://pubs.acs.org
Publication Date (Web): February 18, 2009 | doi: 10.1021/jp8094853

This paper provides an overview of recent research activities concerning the quantum-mechanical description of structures and properties of electronically excited chromophores in solution. The focus of the paper is on a specific approach to include solvent effects, namely the polarizable continuum model (PCM). Such a method represents an efficient strategy if coupled to proper quantum-mechanical descriptions such as the time-dependent density functional theory (TDDFT). As a result, the description of molecules in the condensed phase can be extended to excited states still maintaining the computational efficiency and the physical reliability of the ground-state calculations. The most important theoretical and computational aspects of the coupling between PCM and TDDFT are presented and discussed together with an example of application to the study of the low-lying electronic excited states of push−pull chromophores in different solvents.

1. Introduction

The modeling of excited states formation and relaxation of molecules in solution is a very important issue in many fields of chemistry, biology and physics.[1] The development of accurate but still computationally feasible strategies is a challenging task due to the complexity of the problem in which the processes of formation and relaxation of the electronic states have to be coupled with the dynamics of the solvent molecules. As a consequence, the definition of the excited states of molecular solutes also requires the characterization of the solvent degrees of freedom that are composite in nature and very large in number.

A very well-known example of such a coupling is the distinction between "nonequilibrium" and "equilibrium" solvation regimes following an electronic transition in the solute. The differences in the characteristic response time of the various degrees of freedom of the solvent, in fact, may lead to a solvation regime in which the slow components (i.e., those arising from molecular translations and rotations) are not equilibrated with the excited-state electronic redistribution upon vertical excitation. The resulting nonequilibrium regime will then relax into a new equilibrium in which the solvent is allowed to completely equilibrate, i.e., to reorganize all its degrees of freedom including the slow ones. Especially for highly polar solvents, these two different regimes can influence the properties of the solute excited states in very different ways.

Equilibrium versus nonequilibrium is just one of the specific issues that have to be properly accounted for in the complex task of the definition of realistic and accurate models for the description of structure and properties of excited states in solution.[2] In addition, the necessity of a proper description of different electronic states implies a quantum-mechanical (QM) description. These requirements, together with the generally medium-to-large dimensions of the molecular systems of real interest in this field, are difficult to satisfy when the effect of the environment is also to be included. As a result of this combination of complex aspects, the largest part of the models proposed in the literature introduces a focused approach, i.e., a more accurate description of the molecular system of interest (the chromophore, possibly including small portions of the environment) and a less accurate description of the remainder.

There are different formulations of the focused approach; the most common ones are the hybrid QM/molecular mechanics (QM/MM)[3] and the continuum solvation models.[4−6] Both of them use a classical description for the environment but, whereas in the former the microscopic nature of the solvent molecules is maintained, in the latter a macroscopic dielectric is used. The different philosophy beyond the two classes of methods leads to important differences in both the physical and the computational aspects of their applications, as well as in their range of applicability. The methods based on explicit representations of the environment yield information on specific configurations of the environment around the chromophore, whereas the continuum models give only an averaged picture of it. On the other hand, QM/MM requires many more calculations than continuum models to obtain a correct statistical description. This much larger computational cost of QM/MM is particularly disadvantageous in the study of excited states, as the QM level required is generally quite expensive even for a single calculation on an isolated system; thus, the necessity to repeat the calculation many times makes the approach very expensive (or

* Corresponding author. E-mail: bene@dcci.unipi.it.
† Università di Pisa.
‡ Scuola Normale Superiore.
§ Università di Parma.

10.1021/jp8094853 CCC: $40.75 © 2009 American Chemical Society
Published on Web 02/18/2009

B. Mennucci was born in Lucca, Italy, in 1969. Since 2002 she has been associate professor of physical chemistry at the department of Chemistry of the University of Pisa. She received her "Laurea" degree in chemistry in 1994 and her Ph.D. degree in chemistry from the University of Pisa in 1998 discussing a thesis on theoretical models and computational applications of molecular phenomena involving the environment effect. Her research interests focus on the elaboration of theoretical models and computational algorithms to describe molecular systems in condensed phase with particular attention to molecular properties and time-dependent phenomena. She has authored, or coauthored, about 130 publications.

C. Cappelli was born in Pisa, Italy, in 1972. She received her "Laurea" degree in chemistry in 1998 and her Ph.D. degree in chemistry from the Scuola Normale Superiore, Pisa, Italy, in 2002 discussing a thesis on theoretical models for the calculation of vibrational spectroscopies of molecules in solution. After four years at the Istituto Nazionale per la Fisica della Materia (INFM) as PostDoctoral researcher, in 2006 she became assistant professor at the Department of Chemistry of the University of Pisa. Her research field is theoretical and computational chemistry with particular focus on the modeling of the effects of the environment on response and spectroscopic properties. She has authored, or coauthored, more than 45 publications.

C. A. Guido was born in Tortona, Italy, in 1983. He received his "Laurea" degree in Chemistry in 2007 from the University of Pisa, discussing a thesis on the quantum mechanical models for Resonant Raman Scattering of molecules in solution. He is presently Ph.D. student at the Scuola Normale Superiore of Pisa.

R. Cammi was born in Busseto, Italy, in 1954. In 1979, he was awarded the degree of "Dottore in Chimica" at the University of Parma, discussing a thesis in theoretical chemistry. Since 1983 he has been researcher at the Institute of Physical Chemistry of the University of Parma. In 2000 he became associate professor at the Department of General and Inorganic Chemistry, Analytical Chemistry, Physical Chemistry of the University of Parma, and since 2002 he has been full professor of theoretical chemistry at the University of Parma. He teaches physical chemistry and theoretical chemistry. His research field is theoretical and computational chemistry, mainly the development and application of quantum mechanical continuum methods to the study of solvent effects on molecular processes and properties. He has authored more than 90 publications.

J. Tomasi has spent his entire academic career as a faculty member at the University of Pisa. His research interests cover several aspects of theoretical chemistry with propensity to the formulation and elaboration of models based on ab initio quantum chemistry with a special emphasis on the exploitation of the interpretation of the phenomenon to obtain computational codes of easy use. This approach has been applied to molecular interactions, chemical reaction mechanisms, photochemical processes, solvent effects on molecular response properties, and other related subjects. He has authored, or coauthored, more than 300 scientific papers.

Downloaded by INIST TITAN SCIENCES on September 14, 2009 | http://pubs.acs.org
Publication Date (Web): February 18, 2009 | doi: 10.1021/jp8094853

even not feasible). For this reason, most of the QM/MM calculations on excited states make use of semiempirical QM methods.[7] On the contrary, the level of the QM description can be any when continuum models are used, as the additional cost with respect to gas-phase calculations remains very limited. In addition, continuum solvation models include effects of mutual polarization between the solute and the environment (also those due to a possible nonequilibrium solvation), whereas standard QM/MM methods are based on nonpolarizable force fields. As a matter of fact, QM/MM approaches including environment polarization have been proposed and also applied to the study of excited states of solvated systems.[8] However, among the available approaches, the most popular for this kind of study is still represented by continuum solvation models.[9] In particular, the polarizable continuum model (PCM) developed in Pisa[5] has been shown to give a reliable description of different phenomena involving electronically excited states.[10,11] PCM is in fact a very general continuum model, which has been extended to many different QM levels as well as to QM methods to evaluate energy derivatives with respect to many different perturbations. These extensions have made PCM applicable to calculate geometries and properties of various electronic states as well as to study processes and spectroscopies involving both ground and excited states.

Within the PCM formulation, an important specificity of the extension of QM solvation models to describe excited states has been rigorously analyzed both from a formal and from a numerical point of view.[12] In such an analysis, it has been shown that the application of these models to either linear response (random-phase approximation, RPA,[13] configuration interaction-singles, CIS,[14] and time-dependent density functional theory, TDDFT[15,16] etc.) or state specific approaches (complete active space self-consistent field, CASSCF, configuration interaction CI, etc.) may lead to differences due to an intrinsic nonlinear character of the solvent response operators used in continuum models and in polarizable QM/MM. The state specific (SS) approaches, which are based on the explicit calculation of the excited-state wave function, properly take into account the variation of the solute−solvent interaction accompanying the change of the electronic density during an electronic excitation, whereas the linear response methods introduce only the effects related to the corresponding transition density. To reduce these intrinsic differences, recently some of the authors of the present article have presented a method in which a SS correction is introduced in linear response (LR) approaches.[17] This method is based on the use of the relaxed density, which can be obtained in PCM−LR approaches thanks to their extension to analytical gradients now available not only at CIS[18] but also at TDDFT level.[19]

In the present paper we intend to show that the strategies we have proposed in the years within the PCM framework can be successfully applied to the study of formation and relaxation of excited states in solvated systems. In particular, the coupling of these strategies with the time-dependent density functional theory (TDDFT) can indeed represent an efficient general approach to describe solvent effects on spectroscopies, and more in general on structures and properties of solvated excited states. TDDFT, in fact, can include correlation effects through the exchange−correlation potential for both the ground and the excited states without adding a significant computational effort, whereas PCM can include all required specificities necessary to describe excited states in a formally simple and computationally efficient way. The success of such a coupling is demonstrated by the increasing number of applications; considering only ACS journals, the papers published in the last two years that make use of PCM−TDDFT to describe excitation processes in solvated systems are more than one hundred.

The paper is organized as follows, in the first part a summary of the PCM theoretical tools specifically developed to study excited states is reported and in the second part the same tools are applied to study two molecular systems belonging to the family of push−pull systems. Finally, a summary section with future directions is reported.

2. PCM Tools for Excited States

2.1. Equilibrium vs Nonequilibrium Solvation. When a PCM description is adopted, the molecular system under scrutiny (the solute) is described as a QM charge distribution within a molecular cavity of realistic shape, whereas the environment (the solvent) is described as a structureless polarizable continuum, characterized by its dielectric constants. The solute−solvent electrostatic interactions are described in terms of a new QM operator (solvent reaction potential operator), $\hat{V}_o$, expressed as the electrostatic interaction between the solute and an apparent surface charge density (ASC) on the cavity surface, which describes the solvent polarization in the presence of the solute

Downloaded by INIST TITAN SCIENCES on September 14, 2009 | http://pubs.acs.org
Publication Date (Web): February 18, 2009 | doi: 10.1021/jp8094853

nuclei and electrons. In the computational practice a boundary-element method (BEM) is applied by partitioning the cavity surface into finite elements and by substituting the apparent surface charge density by a collection of point charges q_k, placed at the center of each element s_k, so to obtain

$$\hat{V}_\sigma(\mathbf{r}) = \sum_k \frac{1}{|\mathbf{r} - s_k|} q(s_k;\epsilon,\rho_{GS}) \quad (1)$$

where r is the electronic coordinate and we have indicated the explicit dependence of the apparent charges q on the solvent dielectric constant ϵ and the solute ground-state charge density ρ_{GS} (including the nuclear contribution). Within the PCM framework, over the years different equations have been proposed to define the apparent charges, here we shall adopt the most general one also known as integral equation formalism (IEFPCM).[20]

The PCM energetic functional to be variationally minimized and the QM basic equation become

$$\mathcal{G} = \langle\Psi|\hat{H}^0 + \hat{V}_\sigma|\Psi\rangle - \frac{1}{2}\langle\Psi|\hat{V}_\sigma|\Psi\rangle \quad (2)$$

and

$$\hat{H}_{eff}|\Psi\rangle = [\hat{H}^0 + \hat{V}_\sigma]|\Psi\rangle = E^{GS}|\Psi\rangle \quad (3)$$

where $\hat{H}^0$ is the Hamiltonian for the isolated system.

The free energy expression given in eq 3 for a ground state can be generalized to an excited state K in both an equilibrium and a nonequilibrium solvation regime.

By rewriting the solute electronic density (in terms of the one-particle density matrix **P** on a given basis set) corresponding to the excited state K as a sum of the GS and a relaxation term $\mathbf{P}_\Delta$, and by assuming a linear dependence of the solvent charges (and the reaction potential) on **P**, we obtain

$$\mathcal{G}_K^{eq} = E_{GS}^{K,eq} - \frac{1}{2}\sum_i V_{GS}(s_i)\, q_{GS}(s_i) + \frac{1}{2}\sum_i V(s_i;\mathbf{P}_\Delta)\, q_\Delta(s_i;\mathbf{P}_\Delta) \quad (4)$$

where $V_{GS}(s_i)$ is the electrostatic potential produced by the solute in its ground state on the cavity surface and $E_{GS}^{K,eq}$ is the excited-state energy in the presence of the GS fixed reaction field ($\hat{V}_\sigma$(GS)) and is defined as follows:

$$E_{GS}^{K,eq} = \langle\Psi_K^{eq}|\hat{H}^0|\Psi_K^{eq}\rangle + \sum_i V_K(s_i)\, q_{GS}(s_i) \quad (5)$$

In the above equations a complete equilibration between the solute in the excited state K and the solvent is assumed. In the nonequilibrium regime, eq 4 is replaced by a similar equation, which can be obtained by using two alternative but equivalent, schemes (often associated to the names of Pekar and Marcus).[21] Such two schemes are characterized by a different partition of the slow and fast contributions to the apparent surface charge; all the details of these two partitions can be found in ref 5 (here only what is indicated as Partition II in the reference paper will be used). In such a partition, the slow and fast indices are replaced by the subscripts "in" and "dyn" referring to the "inertial" and "dynamic" solvent polarization, respectively:

$$\mathbf{q}_K^{dyn} = \mathbf{q}_{GS}^{dyn} + \mathbf{q}_\Delta^{dyn} \quad \text{and} \quad \mathbf{q}_K^{in} = \mathbf{q}_{GS}^{in} \quad (6)$$

By using such a partition, we get

$$\mathcal{G}_K^{neq} = E_{GS}^{K,neq} - \frac{1}{2}\sum_i V_{GS}(s_i)\, q_{GS}(s_i) + \frac{1}{2}\sum_i V(s_i;\mathbf{P}_\Delta^{neq})\, q_\Delta^{el}(s_i;P_\Delta^{neq}) \quad (7)$$

which is parallel to what was obtained for the equilibrium case but this time the last term is calculated using the dynamic charges q_Δ^{dyn}.

The vertical transition energy to the excited state K is finally obtained by subtracting the ground-state free energy $\mathcal{G}_{GS}$ to $\mathcal{G}_K^{neq}$:

$$\omega_K^{neq} = \Delta E_{GS}^{K0,neq} + \frac{1}{2}\sum_i V(s_i;\mathbf{P}_\Delta^{neq})\, q_\Delta^{dyn}(s_i;\mathbf{P}_\Delta^{neq}) \quad (8)$$

This equation shows that vertical excitations in solvated systems are obtained as a sum of two terms, the difference between excited- and ground-state energies in the presence of a frozen ground-state solvent ($\Delta E_{GS}^{K0,neq}$) and a relaxation term, which is determined by the mutual polarization of the solute and the solvent after excitation. The latter term is obtained by taking into account the fast and slow partition of the solvent response. In the following section we shall show that this relaxation term is the one leading to differences in the two alternative SS and LR approaches.

2.2. State Specific vs Linear Response. The requirement needed to incorporate the solvent effects into a state-specific method is fulfilled by using the effective Hamiltonian $\hat{H}_{eff}$ defined in eq 3. The only specificity to take into account is that, to calculate $\hat{V}_\sigma$, the density matrix of the electronic state of interest has to be known. Such a nonlinear character of $\hat{V}_\sigma$ is generally solved through an iterative procedure:[22] at each iteration the solvent-induced component of the effective Hamiltonian is computed by exploiting eq 1, with the apparent charges determined from the standard ASC equation with the first-order density matrix of the preceding step. At each iteration n, the free energy of the state K is obtained as

$$\mathcal{G}_K^n = \langle\Psi_K^n|H^0|\Psi_K^n\rangle + \frac{1}{2}\sum_i \langle\Psi_K^n|\hat{V}_\sigma(\Psi_K^{n-1})|\Psi_K^n\rangle \quad (9)$$

where the solvent operator $\hat{V}_\sigma(\Psi_K^{n-1})$ has been obtained using the solute electronic density calculated with the wave function of the previous iteration. At convergence Ψ_K^{n-1} and Ψ_K^n must be the same and eq 9 gives the correct free energy of the state K.

We note that this procedure is valid only for states fully equilibrated with the solvent; the accounting of nonequilibrium requires a two-step calculation: (i) an equilibrium calculation for the initial electronic state (either ground or excited), from which the slow (or inertial) apparent charges, $\mathbf{q}^{in}$, are obtained and stored for the successive calculation on the final state. (ii) A nonequilibrium calculation performed with the interaction potential $\hat{V}_\sigma$ composed of two components, $\hat{V}_\sigma = V_{fixed} + V_{change}$, where V_{fixed} is constant due to the fixed $\mathbf{q}^{in}$ of the previous calculation, and V_{change} changes during the iteration procedure. It is defined in terms of the fast (or dynamic) charges q^{dyn} (see eq 6) as obtained from the charge distribution of the solute final state.

In contrast, the alternative LR approach is solved in a single-step calculation for the whole spectrum of the excited states of interest, similarly to what done for isolated systems.[23,24] Also, for solvated systems we can introduce a TD variational wave function $\Psi(t)$, expressed in terms of the time-independent unperturbed variational wave function $\Psi(t) = \Psi_0 + \nabla\Psi_0 d + ...$ and limit the time-dependent parameter d to its linear term.[13]

Instead of working in terms of time, we then shift to the frequency domain where the linear term in the parameter assumes the form $d = [X \exp(-i\omega t) + Y \exp(i\omega t)]/2$ where the $|\mathbf{X}, \mathbf{Y}\rangle$ vectors are determined by solving the following system:

$$\left[\begin{pmatrix} A & B \\ B^* & A^* \end{pmatrix} - \omega \begin{pmatrix} 1 & 0 \\ 0 & -1 \end{pmatrix}\right]\begin{pmatrix} \mathbf{X} \\ \mathbf{Y} \end{pmatrix} = 0 \tag{10}$$

The quantity in square brackets is the inverse of the linear response matrix for the molecular solute.[24] In eq 10, A and B collect the Hessian components of the free energy functional $\mathbf{G}$ with respect to the wave function variational parameters. The poles ($\pm\omega_K$) of the response function give an approximation of the transition energies of the molecules in solution; the latter are obtained as eigenvalues of the system (10), where $|\mathbf{X}_K, \mathbf{Y}_K\rangle$ are the corresponding transition eigenvectors.

This general theory can be made more specific by introducing the explicit QM level; by using a DFT description, we obtain the time-dependent DFT (TDDFT).[16] Within this formalism, the free energy Hessian terms yield[24,25]

$$A_{ai,bj} = \delta_{ab}\delta_{ij}(\epsilon_a - \epsilon_i) + (ia|jb) + f^{xc}_{ai,bj} - c_x(ab|ij) + \mathcal{V}^{PCM}_{ai,bj} \tag{11}$$

$$B_{ai,bj} = (ia|jb) + f^{xc}_{ai,bj} - c_x\delta_\sigma(ja|ib) + \mathcal{V}^{PCM}_{ai,bj} \tag{12}$$

where $f^{xc}_{ai,bj}$ represents a matrix element of the exchange−correlation kernel in the adiabatic approximation, $(ia|jb)$ indicates two-electron repulsion integrals and ε_r orbital energies. Here we have used the standard convention in the labeling of molecular orbitals, that is, $(i, j,...)$ for occupied and $(a, b,...)$ for virtual orbitals, and we have introduced the hybrid mixing parameter c_x,[26] which allows us to interpolate between the limits of "pure" density functionals ($c_x = 0$, no exact exchange) and HF theory ($c_x = 1$, full exchange and no correlation).

In the definitions (11) and (12) the effect of the solvent acts in two ways: (a) indirectly, by modifying the molecular orbitals and the corresponding orbital energies (they are in fact solutions of the Fock equations including solvent reaction terms), and (b) explicitly, through the perturbation term $\mathcal{V}^{PCM}_{ai,bj}$. This term can be described as the electrostatic interaction between the charge distribution $\psi^*_a\psi_i$ and the dynamic contribution to the solvent reaction potential induced by the charge distribution $\psi^*_b\psi_j$, and it can be written in terms of the vector product between the electrostatic potential and the induced apparent fast charges, determined by the corresponding transition density charge, namely

$$\mathcal{V}^{PCM}_{ai,bj} = \sum_k V_{ai}(s_k) q^{dyn}_{bj} \tag{13}$$

It is now possible to meaningfully compare the excitation energies obtained with the explicit determination of the excited-state wave functions and those given by the LR theory. By comparing the PCM term reported in (8) with the one reported in eq 13, we note that they are formally and physically different; the former depends on the electrostatic potential and PCM charges calculated using the relaxed density matrix $\mathbf{P}_\Delta$ of the excited state, whereas in the latter the same quantities have been obtained by using transition matrix elements. The difference between the two approaches can be clarified by interpreting the excitation in solution as a two-step process: in the first step, the molecule that used to be in its ground state in equilibrium with the solvent is excited to the state K in the presence of a solvent polarization frozen to the value proper for the solute ground state. The energy change related to this process, ($\Delta E^{K0,neq}_{GS}$), is equally described by the two theories. In the second step of the excitation process, the fast degrees of freedom of the solvent rearrange to equilibrate with the charge density of the solute excited state; in this step the two theories diverge because the energy variation accompanying this relaxation is not explicitly accounted for in the LR framework. On the contrary, the LR accounts for a correction which, being originated by the dynamic solute−solvent interactions, might be classified as a part of dispersion.

2.3. Linear Response Approach to a State-Specific Solvent Response. In eq 4 (or equivalently in eq 7 for the nonequilibrium regime) we have shown that excited-state free energies can be obtained by calculating the frozen-PCM energy E^K_{GS} and the relaxation term of the density matrix, $\mathbf{P}_\Delta$ (or $\mathbf{P}^{neq}_\Delta$), where the calculation of the relaxed density matrices requires the solution of a nonlinear problem being the solvent reaction field dependent on such densities.

If we introduce a perturbative scheme and we limit ourselves to the first order, an approximate but effective way to obtain such quantities is represented by the LR scheme as shown in the following equations.

Using a LR scheme, in fact, we can obtain an estimate of $\Delta E^{K0}_{GS} = E^K_{GS} - E^{GS}$, which represents the difference between the excited- and ground-state energies in the presence of a frozen ground-state solvent as the eigenvalue (ω^0_K) of a non-Hermitian eigensystem of type (10), where $\mathcal{V}^{PCM}_{ai,bj} = 0$ but the orbitals and the corresponding orbital energies used to build the $\mathbf{A}$ and $\mathbf{B}$ matrices have been obtained by solving the SCF equation in the presence of a ground-state solvent. By using this approximation, the equilibrium and nonequilibrium free energies for the excited state K become

$$\mathcal{G}^{eq}_K = \mathcal{G}_{GS} + \omega^0_K + \frac{1}{2}\sum_i V(s_i;\mathbf{P}_\Delta)\, q_\Delta(s_i;\mathbf{P}_\Delta) \tag{14}$$

$$\mathcal{G}^{neq}_K = \mathcal{G}_{GS} + \omega^0_K + \frac{1}{2}\sum_i V(s_i;\mathbf{P}^{neq}_\Delta)\, q^{dyn}_\Delta(s_i;\mathbf{P}^{neq}_\Delta) \tag{15}$$

The only unknown term of eqs 14 and 15 is the relaxation part of the density matrix, $\mathbf{P}_\Delta$ (or $\mathbf{P}^{neq}_\Delta$) (and the corresponding apparent charges q_Δ or q^{dyn}_Δ). These quantities can be obtained through the extension of LR approaches to analytical energy gradients (see next section). In these extensions the so-called $\mathbf{Z}$-vector[27] (or relaxed-density) approach is used; as shown in the next section, this approach allows a computationally efficient implementation of the post-HF and TDDFT analytical gradients. The solution of the $\mathbf{Z}$-vector equation as well as the knowledge of eigenvectors $|X_K, Y_K\rangle$ of the linear response system allows one to calculate $\mathbf{P}_\Delta$ for each state K as

$$\mathbf{P}_\Delta = \mathbf{T}_K + \mathbf{Z}_K \tag{16}$$

where $\mathbf{T}_K$ is the unrelaxed density matrix with elements given in terms of the vectors $|X_K, Y_K\rangle$, whereas the $\mathbf{Z}$-vector contribution $\mathbf{Z}_K$ accounts for orbital relaxation effects.

Once $\mathbf{P}_\Delta$ is known, we can calculate the corresponding apparent charges $q^x_\Delta = q(\epsilon_x,\mathbf{P}^x_\Delta)$, where

$$\begin{cases} \epsilon_x = \epsilon \\ \mathbf{P}^x_\Delta = \mathbf{P}_\Delta \\ \mathbf{q}^x_\Delta = \mathbf{q}_\Delta \end{cases} \quad \text{equilibrium;}$$

$$\begin{cases} \epsilon_x = \epsilon_\infty \\ \mathbf{P}^x_\Delta = \mathbf{P}^{neq}_\Delta \\ \mathbf{q}^x_\Delta = \mathbf{q}^{dyn}_\Delta \end{cases} \quad \text{nonequilibrium}$$

By introducing the relaxed density, $\mathbf{P}_\Delta$, and the corresponding charges into eqs 4 (or eq 7), we obtain the first-order ap-

Downloaded by INIST TITAN SCIENCES on September 14, 2009 | http://pubs.acs.org
Publication Date (Web): February 18, 2009 | doi: 10.1021/jp8094853

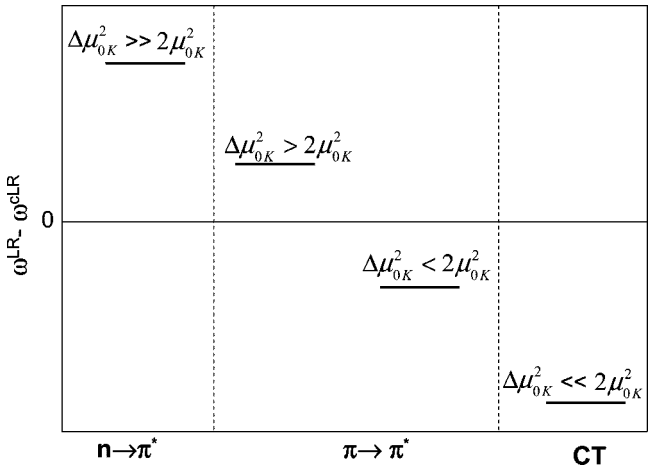

Figure 1. Graphical representation of a qualitative comparison between LR and cLR for some common excitations.

Downloaded by INIST TITAN SCIENCES on September 14, 2009 | http://pubs.acs.org
Publication Date (Web): February 18, 2009 | doi: 10.1021/jp8094853

proximation to the "exact" free energy of the excited state by using a linear response scheme. This is just what we have called "corrected" linear response (cLR) approach.[17] The same scheme has been successively generalized to include higher order effects.[28]

To have a qualitative estimate of the changes in excitation energies one obtains moving from LR to cLR approach, we can adopt the simple diagnostic index formulated in ref 17 using a first-order perturbation theory for a simplified system (a dipole at the center of a spherical cavity). Such an index correlates the correction of the SS and LR approaches with respect to the frozen-solvent transition energy ω_K^0 with state and transition dipoles, namely

$$\frac{\omega_K^0 - \omega_K^{LR}}{\omega_K^0 - \omega_K^{SS}} = \frac{2\mu_{0K}{}^2}{\Delta\mu_{0K}{}^2} \tag{17}$$

where $\Delta\mu_{0K}$ is the difference between the ground- and excited-state K dipole moment and μ_{0K} is the corresponding transition dipole. Obviously, we cannot expect that such a relation based on a spherical cavity and a dipolar coupling between the solute and the reaction field is exactly fulfilled by the PCM values but it is reasonable to suppose that the correlation with $\Delta\mu_{0K}$ and μ_{0K} is maintained. By doing that, we can predict the differences between LR and cLR transition energies for some typical excitations (namely nπ*, $\pi\pi$* and charge transfer) from the graph reported in Figure 1.

As can be seen from the graph, the largest differences are found for transitions in which the difference between the dipole change and the transition dipole is large; in particular, ω_K^{cLR} will be significantly smaller (larger) than ω_K^{LR} if $\Delta\mu_{0K}^2$ is much larger (smaller) than 2 μ_{0K}^2. These two extreme situations typically apply to nπ* and charge-transfer transitions, respectively.

We conclude this section by observing that, even if here it is interesting to emphasize possible differences between the two approaches, it is also important to note that the solvatochromic contribution related to the inertial response of the solvent (i.e., that determining ω_K^0) is described in the same way. With such a contribution being the main part of relative solvatochromic shifts, we can expect that in all cases cLR and the LR approaches will give very similar descriptions of the solvent effect and, in particular, of the relative shift passing from one solvent to the other.

2.4. Analytical Gradients of the Excited State Energy. Once we have described the extension of PCM to LR approaches to evaluate excitation energies, the natural following step is to generalize it to the analytical derivatives with respect to specific perturbations. In this way, in fact, we can extend the study of excited states to their relaxed geometries and properties.

The evaluation of analytical derivatives of the PCM−TDDFT excitation energy ω with respect to the generic parameter (e.g., a nuclear coordinate) ξ has been proposed by Scalmani et al.,[19] as a generalization of the analogous derivative for the PCM−CIS excitation energies.[18] The starting point is the definition of the gradient of the poles of eq 10; this gradient does not require any derivative of the excitation amplitudes (i.e., the eigenvectors) because they have been variationally determined, but it requires the changes in the elements of the Fock matrix. These, in turn, require the knowledge of the MO coefficients derivatives, which are the solution of the couple perturbed Kohn−Sham equations (CPKS).

It has been shown that there is no need to solve the CPKS equations for each perturbation, but rather only for one degree of freedom, which represents the orbital relaxation contribution to the one-particle density matrices (1PDM) involved in all post-SCF gradient expressions.[27] In the resulting equation, the occupied−occupied and virtual−virtual blocks of the $\mathbf{P}^\Delta$ matrix are already available from the diagonalization of (10), whereas the occupied−virtual block is the unknown (see eq 16).

The final form of the gradient of the excitation energy is conveniently expressed in the AO basis as

$$\omega^\xi = \sum_{\mu\nu} h^\xi_{\mu\nu} P^\Delta_{\mu\nu} + \sum_{\mu\nu} S^\xi_{\mu\nu} W_{\mu\nu} + \sum_{\mu\nu\kappa\lambda} (\mu\nu|\kappa\lambda)^\xi \Gamma_{\mu\nu,\kappa\lambda} + \omega^{xc,\xi} + \omega^{PCM,\xi} \tag{18}$$

where we have used μ, ν,... to indicate atomic basis functions, $\Gamma_{\mu\nu,\kappa\lambda}$ to indicate the two-particle density matrix (2PDM), which collects all the contributions that multiply the integral first derivatives $(\mu\nu|\kappa\lambda)^\xi$, and $W_{\mu\nu}$ to indicate the energy weighted density matrix. Here $h^\xi_{\mu\nu}$ and $S^\xi_{\mu\nu}$ are the derivatives of the one-electron Hamiltonian and the overlap matrix, respectively, and $\omega^{xc,\xi}$ is a derivative of exchange−correlation contributions. All the details of the derivation of this expression can be found in the reference paper, here it is useful to focus on the PCM parts only. Equation 18 includes two explicit PCM contributions:

$$\omega^{PCM,\xi} = \sum_{\mu\nu} V^{PCM(\xi)}_{\mu\nu} P^\Delta_{\mu\nu} + \sum_{\mu\nu\kappa\lambda} \mathcal{V}^{PCM(\xi)}_{\mu\nu,\kappa\lambda} (X+Y)_{\mu\nu} (X+Y)_{\kappa\lambda} \tag{19}$$

even if the solvent reaction field also implicitly affects eq 18 through $\mathbf{P}^\Delta$ and $\mathbf{W}$. The first explicit PCM contribution is common to all post-SCF gradients and involves the change in the 1PDM made by the post-SCF procedure:[18]

$$\sum_{\mu\nu} V^{PCM(\xi)}_{\mu\nu} P^\Delta_{\mu\nu} = \sum_{\mu\nu} P^\Delta_{\mu\nu} \left[\sum_k V^E_{\mu\nu,k} q^w_k \right]^{(\xi)} \tag{20}$$

In eq 20, $V^{E,\Delta}_k$ is the change in the solute electronic potential on the cavity surface corresponding to the change in the 1PDM, $V^{E,\Delta}_k = {}_{\mu\nu} P^\Delta_{\mu\nu} V^E_{\mu\nu,k}$. The second explicit PCM contribution to eq 18 is specific to the linear response theory and arises from the derivative of the reaction field matrix element $V^{PCM}_{\mu\nu,\kappa\lambda}$.

Equation 18 can be finally summed to the standard DFT contribution to give the expression for the total free energy gradient of each state in the presence of the solvent, $G^{TDDFT,\xi} = G^{DFT,\xi}_{gs} + \omega^\xi$, where $G^{DFT,\xi}_{gs}$ is the ground-state DFT gradient contribution (see ref 29).

This procedure can be used to obtained excited-state relaxed geometries and emission energies by applying the nonequilibrium description presented in section 2.1, but this time in a

reversed order (i.e., an equilibrated excited state and a non-equilibrium, or vertical, ground state). As a matter of fact, PCM has been also extended to model the TD evolution of solvation (solvation dynamics) following the vertical process of emission. This generalization is based on the use of a complex dielectric permittivity as a function of the frequency, $\epsilon(\omega)$.[30]

3. PCM Study of Push−Pull Systems

In this section we report a PCM study of the structure and properties of the low-lying, intramolecular charge-transfer singlet electronic state of two push−pull chromophores that possess an electron-donating group and an electron-accepting group connected by a conjugated π system, namely julolidine−malononitrile (JM) and indolinedimethine−malononitrile (IDMN).

Both JM and IDMN have been deeply studied by Myers-Kelley and co-workers using UV and resonance Raman (RR) spectroscopies.[32,33] JM has been further analyzed with computational studies by our group[34] and by Guthmuller and Champagne;[35] in both studies a PCM description was introduced to include solvent effects.

Here, a comparative analysis of the two systems is presented; such an analysis will start from the suggestions of the two previous papers[34,35] (namely the need of including solvent effects and the importance of a correct QM description), but it will proceed further by applying the PCM tools described in the previous section. In such a way, the nature of the excited state of interest will be deeply analyzed in terms of both structural and electronic aspects.

3.1. Computational Details. The calculations were performed at the DFT level by using the 6-311G(d,p) basis set. As suggested by a previous paper on JM,[35] the effect of HF exchange has been addressed by considering B3LYP, B3LYP-35, and BHandHLYP hybrid functionals. Although both B3LYP and BHandHLYP are commonly used functionals,[26,36] this is not the case for B3LYP-35, which is a Becke three parameter hybrid functional constructed by the following expression:

$$AE_X^{\text{Slater}} + (1-A)E_X^{\text{HF}} + B\Delta E_X^{\text{Becke}} + E_C^{\text{VWN}} + C\Delta E_C^{\text{LYP}}$$

with A, B, and C being 0.65, 0.585, and 0.81, respectively. In comparison, for the B3LYP functional the values are 0.8, 0.72, and 0.81, respectively. The use of these functionals has been motivated by the expected significant dependence of the excited-state geometries and properties on the amount of Hartree−Fock exchange in the functional (B3LYP, BHandHLYP, and B3LYP-35 contain 20%, 50%, and 35% of Hartree−Fock exchange, respectively).

In addition, a fourth functional has been used to test the reliability of DFT hybrid functionals against a proper description of charge-transfer electronic transitions. It has, in fact, being pointed out that standard TDDFT can yield substantial errors for these CT states; these errors have also been attributed to the wrong long-range behavior of the applied standard xc-functionals.[37] To improve the accuracy of CT excitations, while maintaining good quality local excitations, a proposal has been that of partitioning the $1/r$ operator in the exchange term into short- and long-range components.[38] Short-range exchange is then treated primarily using a local functional; long-range exchange is treated primarily using exact orbital exchange. Here in particular, we shall adopt one of this new functionals, the so-called Coulomb-attenuated (CAM-B3LYP)[39] functional, which contains just 19% exact exchange at short-range, like a conventional hybrid, but 65% at long-range.

Solvent effects were described by exploiting the IEFPCM[20] with a molecule-shaped cavity made of interlocking spheres centered on heavy atoms: the default set of sphere radii (UA0) implemented in the Gaussian code was exploited. Vertical excitation energies were obtained in the nonequilibrium solvation regime, by exploiting both the linear response (LR) and the corrected LR (cLR) schemes as described in sections 2.2 and 2.3. Excited-state geometries and properties were obtained applying the TDDFT gradients implementation to all four functionals; see section 2.4. Resonance Raman spectra in solution were obtained by exploiting the extension of IEFPCM to STD approach.[34] All QM calculations were performed using a development version of the Gaussian package[40] whereas the vibronic structure of absorption spectra was simulated by exploiting the FCfast code.[41]

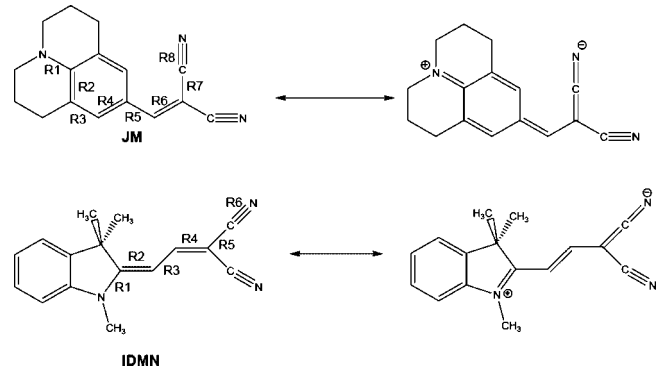

Figure 2. Structure of julolidine−malononitrile (JM) and indolinedimethine−malononitrile (IDMN) in terms of the two resonance forms. The indication of selected bond distances is also given.

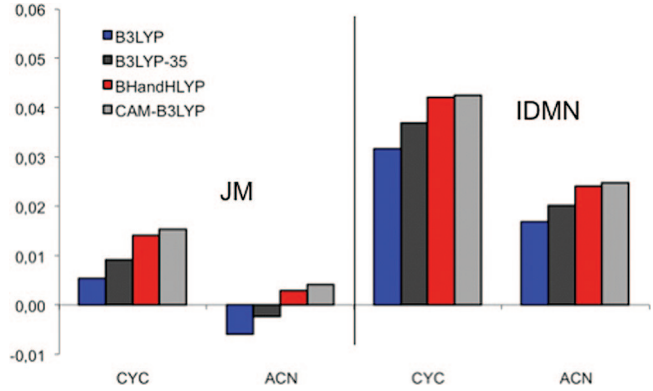

Figure 3. Variations of the BLA index for IDMN and JM moving from cyclohexane (CYC) to acetonitrile (ACN), as obtained by using the four selected DFT functionals.

3.2. Ground-State Structures and Properties. Before moving to the study of excitation and excited-state geometries and properties, let us focus on ground-state geometry and electronic charge distribution.

A key geometrical parameter useful to rationalize the behavior of push−pull systems is the bond length alternation (BLA) index;[42] such an index, which is defined as the difference between the average length of the carbon−carbon single and double bonds, has been widely used in the literature focusing on the structure and properties of push−pull systems (see, e.g., ref 31). By definition, a positive BLA value is associated to the neutral form, a negative value to the zwitterionic form and a zero value to a delocalized system (see Figure 2):

In Figure 3 the variations of BLA for IDMN and JM moving from cyclohexane to acetonitrile are reported, as obtained by using the four DFT functionals.

The values reported are qualitatively consistent with a two-state model, pictorially represented in Figure 2. More specifi-

Downloaded by INIST TITAN SCIENCES on September 14, 2009 | http://pubs.acs.org
Publication Date (Web): February 18, 2009 | doi: 10.1021/jp8094853

TABLE 1: Dipole Moment (Debye) and Isotropic Static Polarizability (Å^3) for the Two Molecules in the Two Solvents As Obtained with Different Functionals

	μ		α	
	CYC	ACN	CYC	ACN
	JM			
B3LYP	13.7	17.3	39.3	50.3
B3LYP35	13.4	16.7	37.6	47.8
BHandHLYP	13.0	16.1	36.2	45.7
CAM-B3LYP	12.2	15.9	37.1	47.1
	IDMN			
B3LYP	12.3	15.4	39.2	48.5
B3LYP35	12.3	15.3	37.6	46.2
BHandHLYP	12.3	15.2	36.3	44.3
CAM-B3LYP	12.0	15.1	37.3	45.8

cally, as the solvent polarity increases, the ground state displays a more zwitterion-like structure: with increasing solvent polarity and increasing zwitterionic character, we observe alternate positive and negative variations of the single and of the double bond lengths along the whole skeleton going from the amino to the cyano nitrogen. The expected solvent dependence of the conjugated bond lengths is easily deduced by inspection of the resonance forms in Figure 2. This behavior is almost identical at each DFT level of description.

In more detail, as can be seen from the inspection of Figure 3, an increase in the BLA index is noticed by increasing the HF exchange percentage in the DFT functional, i.e., going from B3LYP to B3LYP-35, BHandHLYP, and CAM-B3LYP. Such a behavior is common both to cyclohexane and to acetonitrile. A greater HF exchange percentage yields more localized single and double bonds.

Despite this common behavior of BLA, the two chromophores show a different response to the solvent. IDMN is described as a neutral structure in the ground state in both solvents with an increasing delocalization of charge in the polar solvent, as expected. This is not the case of JM that is described as more delocalized than IDMN as shown by the small BLA values (for B3LYP and B3LYP-35 a slightly zwitterion character appears in acetonitrile). It has to be noted that for IDMN the presence of an aromatic ring probably makes the two-state picture not appropriate to rationalize the behavior of this molecule, because the zwitterionic form breaks the aromaticity.

In Table 1, molecular dipole moments and isotropic (electronic) static polarizabilities are reported, as a function of the DFT functional both in cyclohexane and in acetonitrile.

For both molecules, the molecular dipole moment and the polarizability increases going from apolar to polar solvent, as expected, and decreases by increasing the HF exchange percentage in the functional. Once again, some differences appear in the two molecules. For IDMN the effects on the dipole moment due to the change in the functional are less evident than for the previously analyzed geometrical parameters (the largest variation of μ is only of about 2%). IDMN isotropic polarizabilities are slightly more sensitive yielding 4% largest variation going from B3LYP to CAM-B3LYP. For JM, the molecular dipole moment decreases of about 11% moving from B3LYP to CAM-B3LYP, while the static polarizability decreases of about 6%.

In both cases, these data are in agreement with the structural changes reported in the previous section: both dipole moments and polarizabilities increase as the BLA index decreases, i.e., as a more delocalized structure is present.

3.3. Vertical Transition Energies. Before analyzing excited-state structure and properties, let us start the discussion on the transition properties.

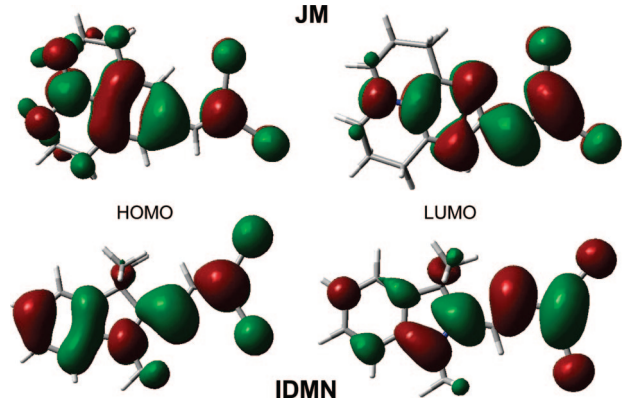

Figure 4. Pictorial view of the HOMO and LUMO orbitals of JM and IDMN.

As said before, we will focus on the first charge-transfer singlet transition, which has a $\pi\pi^*$ character and is described as HOMO−LUMO for all functionals and both systems (see Figure 4).

In Table 2 vertical excitation energies in the two solvents as obtained within both the LR and the cLR frameworks are reported. To have a better appreciation of the LR and cLR differences, the common starting energy ($\Delta E_{GS}^{K0,neq}$) obtained in a frozen ground-state solvation is also reported (see section 2.2 for details).

In general, for both molecules, a decrease in the transition energy value is observed with increasing solvent polarity and such a behavior is common to both LR and cLR. Absolute energies always increase upon passing from LR to cLR. This can be explained using the simple but still effective diagnostic index introduced in eq 17 in terms of differences of dipoles and transition dipoles. As we shall show in the next section, both JM and IDMN present an increase of the dipole moment in the excited state of the order of 3−4 Debye; by using these values and the transition dipoles reported in Table 2, we see that the parameter is much larger than one for both systems: this means that $\Delta E^{LR} < \Delta E^{cLR}$. As this increase is similar in both solvents, the solvatochromic shifts remain almost the same passing from LR to cLR.

Moving to the comparison with experiments, the absolute energies are always overestimated, whereas solvatochromic shifts are reproduced pretty well by all functionals, especially by CAM-B3LYP. The overestimation of the absolute energies is surely due to a combination of different effects, including those related to the use of a continuum electrostatic only solvation model and more important to the use of a TDDFT description. To have an idea of the effect of the QM level, we have compared gas-phase TDDFT results with that obtained at SAC-CI level,[43] which is an accurate method to predict transition energies. For IDMN, all functionals overestimate the SACCI value of about 0.3, 0.5, 0.7 and 0.6 eV for B3LYP, B3LYP-35, BHandHLYP, and CAM-B3LYP, respectively. If we assume that the intrinsic error due to TDDFT is not dependent on the solvent, we can subtract the TDDFT-SACCI differences from the energies reported in Table 2 to obtain effective energies; with that, a good agreement with experiments is recovered, especially for CAM-B3LYP/cLR.

It is also interesting to comment further on the difference between B3LYP and CAM-B3LYP. To do that, we will apply the analysis recently proposed by Peach et al.,[44] where the assessment of the performance of B3LYP, and CAM-B3LYP exchange−correlation functionals for the calculation of local,

Downloaded by INIST TITAN SCIENCES on September 14, 2009 | http://pubs.acs.org
Publication Date (Web): February 18, 2009 | doi: 10.1021/jp8094853

TABLE 2: Excitation Energies (eV) for the Two Molecules in the Two Solvents As Obtained with Different Functionals[a]

	$\Delta E_{GS}^{K0,neq}$		LR			cLR		
	CYC	ACN	CYC	ACN	shift	CYC	ACN	shift
				JM				
B3LYP	3.27	3.21	3.09 (9.20)	3.04 (9.23)	−0.05	3.22	3.17	−0.05
B3LYP35	3.43	3.35	3.28 (9.04)	3.21 (9.23)	−0.07	3.42	3.34	−0.08
BHandHLYP	3.62	3.51	3.46 (8.96)	3.37 (9.18)	−0.09	3.59	3.50	−0.09
CAM-B3LYP	3.50	3.40	3.35 (8.96)	3.25 (9.19)	−0.10	3.48	3.38	−0.10
exp			2.84	2.72	−0.12			
				IDMN				
B3LYP	3.37	3.32	3.22 (9.25)	3.19 (9.17)	−0.03	3.36	3.32	−0.04
B3LYP35	3.57	3.52	3.41 (9.29)	3.39 (9.24)	−0.02	3.56	3.52	−0.04
BHandHLYP	3.76	3.71	3.60 (9.28)	3.56 (9.24)	−0.04	3.75	3.70	−0.05
CAM-B3LYP	3.63	3.58	3.47 (9.32)	3.43 (9.30)	−0.04	3.62	3.57	−0.05
exp			2.90	2.85	−0.05			

[a] In parentheses, transition dipoles are also reported (Debye). Where available, experimental values[32,33] are reported.

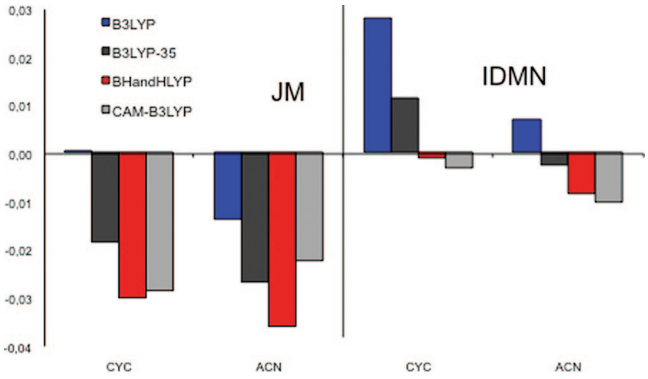

Figure 5. Variation of the BLA index following the excitation for JM and IDMN in cyclohexane (CYC) and acetonitrile (ACN). The four selected DFT functionals are considered.

TABLE 3: Vertical and Relaxed Excited-State Dipoles (Debye) for the Two Molecules in the Two Solvents As Obtained with Different Functionals

	vertical		relaxed	
	CYC	ACN	CYC	ACN
		JM		
B3LYP	17.56	20.08	17.59	21.46
B3LYP35	17.08	19.61	17.42	21.51
BHandHLYP	17.07	19.48	17.28	21.42
CAM-B3LYP	17.14	19.45	17.38	21.60
		IDMN		
B3LYP	15.66	18.63	16.70	20.06
B3LYP35	14.93	17.68	16.17	19.37
BHandHLYP	14.74	17.27	15.45	18.54
CAM-B3LYP	14.86	17.20	15.02	18.05

Downloaded by INIST TITAN SCIENCES on September 14, 2009 | http://pubs.acs.org
Publication Date (Web): February 18, 2009 | doi: 10.1021/jp8094853

Rydberg, and intramolecular CT excitation energies was quantified in terms of a numerical factor ($0 < \Lambda < 1$), which measures the extent to which excitation energy errors correlate with the spatial overlap between the occupied and virtual orbitals. In particular, a small value of Λ signifies a long-range excitation (which should be better described by CAM-B3LYP), whereas a value closer to 1 is related to a short-range excitation (which should be well described by B3LYP). The calculation of the Λ index for JM and IDMN with the two (B3LYP and CAM-B3LYP) functionals shows in all cases values that vary between 0.65 and 0.75, i.e., in the window of values where B3LYP give reliable results.[44]

3.4. Excited-State Structure and Properties. Let us analyze structural changes of the charge-transfer state following the vertical excitation by using, once more, the BLA index (see Figure 5).

For both molecules, the BLA index for the excited state shows an inverse behavior with respect to the ground state. In both solvents the JM excited state is described as a zwitterion by all functionals (BLA < 0) with the exception of B3LYP in cyclohexane, which gives a small positive BLA. Also, for IDMN a negative BLA is found in both solvents with BHandHLYP and CAM-B3LYP, whereas B3LYP35 in cyclohexane and B3LYP in both solvents give positive and not negligible BLA. From this analysis, it is evident that B3LYP fails at describing structural changes upon excitation, whereas the correct picture is recovered either by increasing the percentage of exact exchange (as in BHandHLYP) or by separating out the short and long-range contributions (as in CAM-B3LYP). Also, B3LYP-35 introduces significant improvement in the description of the excited-state geometry with respect to B3LYP; however, such an improvement is not sufficient to get the correct picture for IDMN.

To characterize the excited states also from the electronic point of view, in Table 3 excited-state dipole moments obtained at GS minimum geometry (vertical) and at relaxed geometry for both molecules are reported. This allows us to obtain information on the role played by structural and electronic changes resulting from the electronic excitation.

The inspection of the table shows that the major contribution to the change in the dipole moment passing from ground to excited state results from the vertical excitation: the excited-state nuclear relaxation causes only a further slight increase in the dipole moment. This is particularly true for JM in cyclohexane, where the "vertical" dipole is almost equal to that at the excited-state geometry. We recall that in acetonitrile, in addition to the different geometry, the "relaxed" values distinguish from the vertical ones in the solvation regime used, namely nonequilibrium in the vertical and equilibrium in the relaxed.

The effect of the different functional is quite small especially for JM, but some trends can be observed. Looking first to vertical values, we see that in both molecules the increase of exact exchange (passing from B3LYP to B3LYP-35 and BHandHLYP) leads to smaller dipole moments. This decrease is counterbalanced by the separation between short- and long-range exchange introduced in CAM-B3LYP. If the effect of the functional on the geometry is also considered using the relaxed dipole moments, we see a different behavior for the two molecules. For JM, all functionals are quite similar, whereas for IDMN, B3LYP gives much larger dipole moments than the

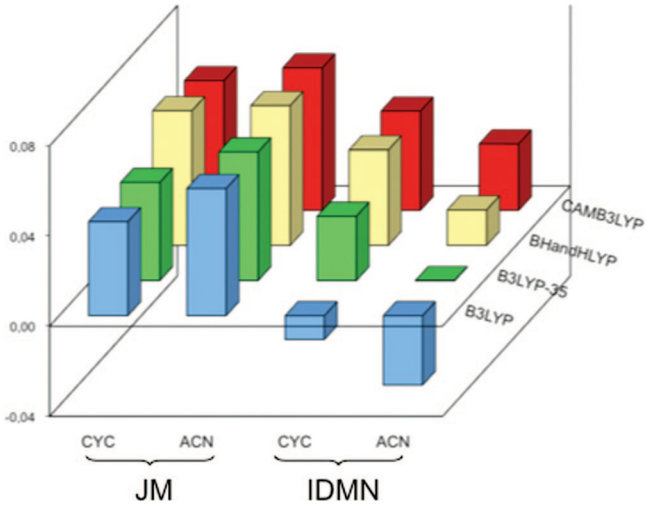

Figure 6. f_{CT} parameter (see text) for JM and IDMN in cyclohexane (CYC) and acetonitrile (ACN) with the four selected DFT functionals.

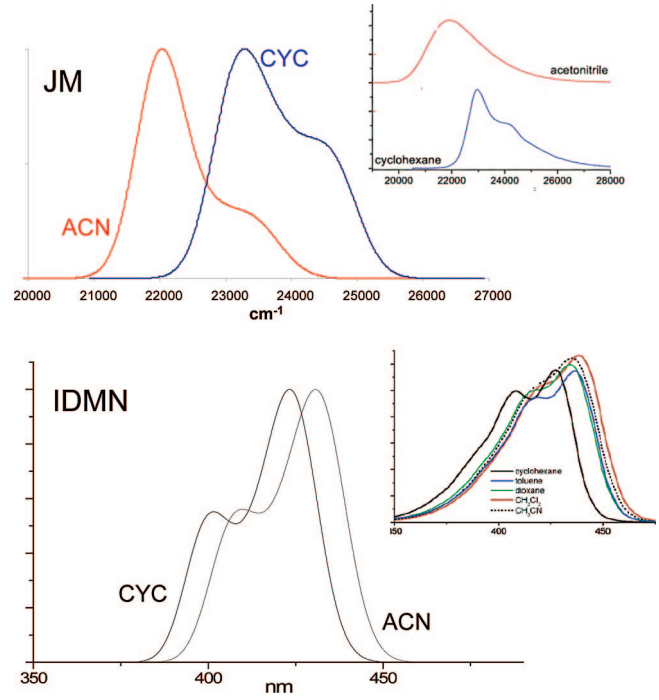

Figure 7. CAM-B3LYP simulated absorption spectra for JM and IDMN as obtained by combining calculated excitation energies with Franck−Condon integrals. Experimental findings taken from ref 32.

other functionals. This unique behavior of B3LYP is a direct consequence of what already commented for BLA reported in Figure 5.

A final analysis of the change in the state character upon excitation can be obtained in terms of a population analysis. Here the Merz−Kollman (MK) model is adopted[46] by using both the vertical and the relaxed excited-state geometries. To have a more direct analysis, it is convenient to define a CT parameter as

$$f_{CT} = \Delta_D^{exc\text{-}gs} - \Delta_A^{exc\text{-}gs}$$

where $\Delta_X^{exc\text{-}gs}$ is the difference of charge in the donor or acceptor unit upon excitation. If the excitation really corresponds to a CT from donor to acceptor, then $\Delta_D^{exc\text{-}gs}$ is large and positive and $\Delta_A^{exc\text{-}gs}$ is still large in absolute value but negative. As a result, f_{CT} will be large and positive. To calculate f_{CT}, we have to define the donor and acceptor units; in both molecules we have assumed the ring nitrogen atom as the donor and the $C(CN)_2$ as the acceptor. The results obtained are reported in Figure 6 for all the functionals and the two solvents.

Once again JM and IDMN present quite different behavior: for JM f_{CT} is always positive and increases with the solvent (by increasing the percentage of HF exchange we observe only a small increase). In contrast, for IDMN the effect of the functional is more dramatic as f_{CT} changes sign by increasing the HF exchange. From this graph it is evident that the excitation in JM presents a much more pronounced CT character than IDMN; in IDMN the excited-state character strongly depends on the functional used and in particular on the percentage of HF exchange but also on the separation into short and long-range terms. Note that B3LYP always predicts a reversed flow of charge from the expected acceptor to the donor (i.e., $f_{CT} < 0$).

To conclude the analysis, we will combine the results obtained so far for JM and IDMN ground- and excited-state structures/properties and use them to simulate UV and Resonance Raman (RR) spectra.

In Figure 7 the simulated absorption spectra are reported; these are obtained by calculating the Franck−Condon integrals of vibrational wave functions belonging to two different electronic states as implemented into the program FCFAST. Experimental findings taken from refs 32 and 33 are also shown as insets. The simulation of the band shapes was done by using CAM-B3LYP ground- and excited-state geometries and ground-state harmonic frequencies (which are assumed to be valid also for the excited state), and a bandwidth of 500 cm^{-1}. This value was taken to reproduce the experimental broadening of the spectrum. So to have a more direct comparison with experimental graphs, spectra are reported in cm^{-1} for JM and in nm for IDMN.

For both molecules the agreement between calculated and experimental findings is satisfactory, the relative intensities of the secondary peak (actually a shoulder) correctly decreases by increasing the solvent polarity exactly as in the experimental spectra. Notice, however, that, because simulated spectra are normalized with respect to the absorption maximum, nothing can be said about the main peak intensity passing from one solvent to the other.

Moving now to RR spectra, the main effects of the solvent (position of the peaks and their intensities) can be ascribed to two different origins: one due to the solvent-induced changes in the geometry of both ground and excited states and the other due to the variations induced in the electronic distribution of both states. As far as concerns the theoretical aspects related to the implementation of PCM−RR, the interested reader can find all the details in ref 34; here we shall only recall that the application of PCM to the two computational strategies commonly used to simulate resonance Raman spectra (the transform theory, TT, approach by Peticolas and Rush[47] and the short-time dynamics, STD, theory[48]) involves the determination of a different portion of the potential energy surface (PES) for the solvated excited state together with a different solvation regime. Namely, in TT an equilibrium solvation and a completely relaxed geometry is used to describe the excited state, whereas in STD the vertical (or Franck−Condon) portion of the excited-state PES is used together with a nonequilibrium solvation. These differences in the treatment of the solvent effect suggests that the STD approach is more suited than TT to describe the sequence of fast events occurring in the Resonance Raman

Downloaded by INIST TITAN SCIENCES on September 14, 2009 | http://pubs.acs.org
Publication Date (Web): February 18, 2009 | doi: 10.1021/jp8094853

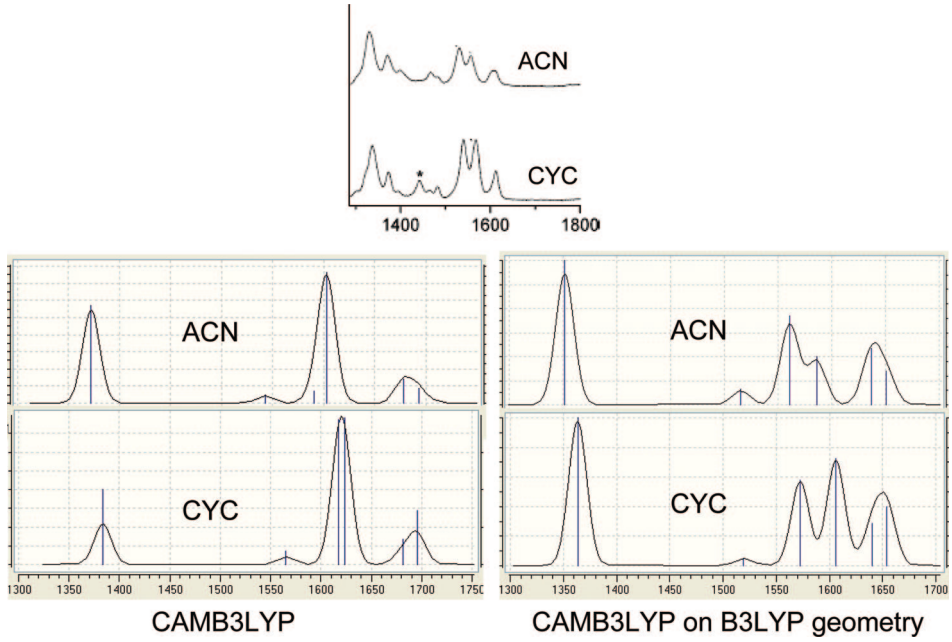

Figure 8. Calculated IDMN RRS spectra in the 1300−1800 cm^{-1} range obtained in the STD-cLR approach in cyclohexane (CYC) and acetonitrile (ACN). Experimental spectra taken from ref 33 are also shown as insets.

Downloaded by INIST TITAN SCIENCES on September 14, 2009 | http://pubs.acs.org
Publication Date (Web): February 18, 2009 | doi: 10.1021/jp8094853

experiments of solvated systems. An analysis of the effects of these different solvation regimes determining TT and STD spectra of JM can be found in the cited paper. The same molecular system has bee further analyzed in a successive paper by Guthmuller and Champagne,[35] where a detailed analysis of the effects of different DFT functionals is reported.

Starting from the results of these studies on JM, here it is of interest to focus on IDMN. As said above, the STD better represents the solvation effects on RR spectra; therefore, in the present study the analysis will be limited to STD intensities, which are defined as[45]

$$I_{0\rightarrow 1_m}(\omega_m) \propto {\omega_m}^2 {\Delta_m}^2; \qquad \Delta_m = \sqrt{\frac{\omega_m}{\hbar}}\Delta Q_m$$

where Δ_m and ΔQ_m are the dimensionless displacement and the displacement along the mass-weighted normal coordinate for mode m (whose vibrational frequency in the ground state is ω_m), respectively. In the STD framework, ΔQ_m is calculated from the partial derivative of the excited-state electronic energy (E_K) along the normal mode Q_m at the ground-state equilibrium position

$$\Delta Q_m = -\frac{1}{{\omega_m}^2}\left(\frac{\partial G_K}{\partial Q_m}\right)_0$$

G_K is the free energy of the K state, obtained through eq 15 within the corrected linear response approach in the nonequilibrium solvation regime.

For the ground-state geometry and frequencies we have used two different functionals, namely CAM-B3LYP and B3LYP, whereas for excited-state gradients only CAM-B3LYP has been used: this functional in fact has shown to be the most reliable method to describe IDMN excited state. Notice that only six normal modes were selected, the ones showing the largest variations upon solvation. The corresponding 1300−1800 cm^{-1} window of the STD-cLR RR spectra is reported in Figure 8 for both solvents (in the inset the experimental spectra are also shown).

The mode at about 1360 cm^{-1} mainly involves the R1 and R4 bond stretching; the peak at about 1520 cm^{-1} is due to the asymmetric stretching mode of the rings. The normal modes yielding peaks at 1570 and 1606 cm^{-1} have similar vibrational components, and in particular the first normal mode involves the in-phase R1 and R4 stretching with out-of-phase R2 and R3 stretching; the second mode is composed of the in-phase R2 and R4 and out-of-phase R3 stretching. The other two normal modes (at about 1640 and 1650 cm^{-1}) both involve the benzene ring stretching, and the one at 1650 cm^{-1} also accounts for the out-of-phase R2 and R3 stretching.

Moving to the comparison with experiments, the main experimental features passing from one solvent to the other are correctly reproduced only by the CAM-B3LYP description using the B3LYP ground-state geometry (and vibrational frequencies). Only at this level of description we reproduce the experimentally observed change in the relative intensities of the peaks in the 1500−1600 region of the spectra. These two peaks are assigned to modes having dominant contributions from the R2 and R4 stretches. These are double bonds in the neutral structure but single bonds in the zwitterion, which should make a larger contribution to the structure in polar solvents. The better agreement obtained with mixed description seems to indicate that CAM-B3LYP gives a less accurate description of the peak position and thus of the ground-state geometry with respect to B3LYP whereas it well describes the nature of the excited state. Such an agreement is not unexpected in light of what has previously been discussed about structural and electronic parameters of the ground and excited states. In fact, although B3LYP gives a good description of the ground state (see, e.g., the discussion on BLA index and vibrational frequencies), CAM-B3LYP is instead more reliable in describing the excited state. In fact, only CAM-B3LYP (and BHandHLYP) give the correct BLA index behavior in the excited state and the corresponding description in terms of charge-transfer character, as evaluated by means of the Merz−Kollman population analysis.

These results show that the correct description of RR spectra, which requires the accurate description of the ground- and

Downloaded by INIST TITAN SCIENCES on September 14, 2009 | http://pubs.acs.org
Publication Date (Web): February 18, 2009 | doi: 10.1021/jp8094853

excited-state PES, is particularly challenging for TDDFT, so that the use of different functionals and/or basis sets, specifically tailored to the states under examination may be required.

4. Summary and Future Directions

In this article we have reviewed recently developed computational tools to study structures and properties of excited-state chromophores in homogeneous solutions. These tools are based on the combination of the polarizable continuum model, the implicit solvation model developed in Pisa since 1981, and the TDDFT approach. The main reason leading to such a combination is of computational nature; in fact, continuum models and TDDFT represent two very general and efficient approaches to describe solvent effects and excited states, respectively. In addition, the combination of PCM and TDDFT presents some more fundamental advantages, as it allows us to easily include all those aspects that are necessary anytime the formation and relaxation of excited states have to be modeled in the presence of a polarizable environment. The PCM−TDDFT scheme in fact includes (i) the formulation of equilibrium and nonequilibrium solvation regimes within the framework of the relaxed density matrix, (ii) the analytical gradient theory for excited states, within the linear response (LR) approximation, and (iii) a modification in the basic LR method that introduces state specific (SS) characteristics but still keeps both its formal simplicity and computationally efficiency.

The applications we have presented show potentialities and limits of this scheme to probe structures and properties of excited states of solvated chromophores, which can now be studied from their formation from a vertical electronic transition within a nonequilibrium solvation regime up to their decay, or relaxation, using a detailed QM description coherently coupled with the dynamics of the solvent. As a matter of fact, further extensions of the same scheme have been presented by our group and by others. Here, it is interesting to recall the extension of PCM−TDDFT to describe the electronic coupling characterizing excitation-energy transfers (EET) among solvated chromophores,[49] or the simulation of line widths and shapes.[50] Another direction of possible extensions of the scheme involves the inclusion of environments of increasing complexity such as gas/liquid and liquid/liquid intefaces[51] and membranes and nanoscopic metal particles.[52]

Further extensions of the PCM methodology to study phenomena involving excited electronic states are also expected in the near future, both to overcome some actual limitations and to expand the variety of phenomena to be studied. For example, the SS-corrected LR approach is now limited to the energy evaluation for single point calculations, and it would desirable to extend this method to include the analytical gradient, so to be able to compute excited-state equilibrium geometries at this level of theory. In addition, at present only electrostatic solvent effects are included in the model; this is a clear approximation that is realistic in polar environments whereas, as soon as the solvent polarity decreases, further nonelectrostatic effects such as repulsion and dispersion can become important especially when considering excited states.

Another progress to achieve is the improvement in the QM level of description. The merits and limits of the TDDFT in describing excited states are well-known; in the present context it is particularly important to recall the deficiency of TDDFT in describing excited states of charge-transfer nature, as these are the states that are expected to undergo large solvent effects. In these cases, there would be the need to go beyond the TDDFT and combine PCM with other more stable QM methodologies, such as those based on a coupled-cluster wave function.

To conclude this article, we cannot forget to recall that all the methodologies we have presented and those we have indicated as possible future extensions, are within the continuum framework. This is indeed an approximation in which all the microscopic aspects of the environment are neglected. Recent studies have shown that in many cases this apparently crude approximation properly compares with methods based on the explicit treatment of the environment molecules (such QM/MM) if a refined version of continuum models is used.[53] Obviously, this is true in the cases in which we do not have strong specific intermolecular interactions between the system of interest and the environment or when these interactions are averaged out in the measurement process. In all the other cases, in fact, a purely continuum approach does not manage to obtain the complete picture of the environment effects. Also in these difficult cases, however, the continuum approach can still represent a simple and effective way to take into account the "mean field" part of the environment effect whereas all the short-range interactions which do not average can be introduced using a "supermolecule" or "cluster" picture. This combined approach in which three different shells are involved (the molecular system under study, the strongly interacting environment molecules and the rest) is indeed very powerful as it accounts not only for both short- and long-range effects but can also be easily extended to explicitly include mutual polarization among the various shells once the explicit additional molecules are treated at QM level or using a polarizable force field. In addition, the same approach can be extended to a real dynamic description in which the molecular degrees of freedom of the system of interest are coupled to those of the strongly interacting environment in the presence of the mean field of the remainder. Both these aspects become particularly important when we want to simulate the formation and relaxation of excited states.

References and Notes

(1) (a) Reichardt, C. *Solvents and Solvent Effects in Organic Chemistry*; Wiley-VCH: Weinheim, 2003. (b) Wang, C. H. *Spectroscopy of condensed media*; Academic Press: New York, 1985. (c) Shukla, M. K., Leszczynski, J., Eds. *Radiation Induced Molecular Phenomena in Nucleic Acids*; Springer: Berlin, 2008. (d) Douhal, A., Santamaria, J., Eds. *Femtochemistry and Femtobiology: Ultrafast Dynamics in Molecular Science*; World Scientific: Singapore, 2002.

(2) (a) Olivucci, M. *Computational photochemistry*; Theoretical and Computational Chemistry; Elsevier: Amsterdam, 2005; Vol. 16. (b) Persico, M.; Granucci, G. *Photochemistry in Condensed Phase in Continuum solvation models in chemical physics, from teory to applications*; Mennucci, B., Cammi, R., Eds.; Wiley: Chichester, U.K., 2007.

(3) (a) Warshel, A.; Levitt, M. *J. Mol. Biol.* **1976**, *103*, 227. (b) Thole, B. T.; van Duijnen, P. Th. *Chem. Phys.* **1982**, *71*, 211. (c) Singh, U. C.; Kollman, P. A. *J. Comput. Chem.* **1986**, *7*, 718. (d) Field, M. J.; Bash, P. A.; Karplus, M. *J. Comput. Chem.* **1990**, *11*, 700. (e) Gao, J. *J. Phys. Chem.* **1992**, *96*, 6432. (f) Thompson, M. A. *J. Phys. Chem.* **1996**, *100*, 14492.

(4) (a) Tomasi, J.; Persico, M. *Chem. Rev.* **1994**, *94*, 2027. (b) Cramer, C. J.; Truhlar, D. G. *Chem. Rev.* **1999**, *99*, 2161.

(5) Tomasi, J.; Mennucci, B.; Cammi, R. *Chem. Rev.* **2005**, *105*, 2999.

(6) Mennucci, B., Cammi, R. , Eds. *Continuum solvation models in chemical physics, from teory to applications*; Wiley: Chichester, U.K., 2007.

(7) (a) Gao, J. *J. Am. Chem. Soc.* **1994**, *116*, 9324. (b) Rajamani, R.; Gao, J. *J. Comput. Chem.* **2002**, *23*, 96. (c) Coutinho, K.; Canuto, S. *J. Chem. Phys.* **2000**, *113*, 9132. (d) Coutinho, K.; Canuto, S.; Zerner, M. C. *J. Chem. Phys.* **2000**, *112*, 9874.

(8) (a) Kongsted, J.; Osted, A.; Mikkelsen, K. V.; Astrand, P. O.; Christiansen, O. *J. Chem. Phys.* **2004**, *121*, 8435. (b) Jacob, C. R.; Neugebauer, J.; Jensen, L.; Visscher, L. *Phys. Chem. Chem. Phys.* **2006**, *8*, 2349. (c) Ohrn, A.; Karlstrom, G. *Mol. Phys.* **2006**, *104*, 3087. (d) Lin, Y. L.; Gao, J. L. *J. Chem. Theory Comput.* **2007**, *3*, 1484.

(9) (a) Karelson, M. M.; Zerner, M. C. *J. Am. Chem. Soc.* **1990**, *112*, 9405. (b) Kim, H. J.; Hynes, J. T. *J. Chem. Phys.* **1992**, *96*, 5088. (c) Pappalardo, R. R.; Reguero, M.; Robb, M. A.; Frisch, M. *Chem. Phys. Lett.* **1993**, *212*, 12. (d) Klamt, A. *J. Phys. Chem.* **1996**, *100*, 3349. (e) Christiansen, O.; Mikkelsen, K. V. *J. Chem. Phys.* **1999**, *110*, 8348. (f) Li, J.; Cramer, C. J.; Truhlar, D. G. *Int. J. Quantum Chem.* **2000**, *77*, 264. (g)

Cossi, M.; Barone, V. *J. Chem. Phys.* **2000**, *112*, 2427. (h) Guillaume, M.; Champagne, B.; Zutterman, F. *J. Phys. Chem. A* **2006**, *110*, 13007. (i) Ferrighi, L.; Frediani, L.; Fossgaard, E.; Ruud, K. *J. Chem. Phys.* **2007**, *127*, 244103.

(10) (a) Mennucci, B. Continuum models for excited states. In *Continuum solvation models in chemical physics, from theory to applications*; Mennucci, B., Cammi, R., Eds.; Wiley: Chichester, U.K., 2007; pp 110. (b) Cammi, R.; Mennucci, B. Structure and properties of molecular solutes in electronic excited states: a Polarizable Continuum Model approach based on the time-dependent density functional theory. In *Radiation Induced Molecular Phenomena in Nucleic Acids: A Comprehensive Theoretical and Experimental Analysis*; Shukla, M. K., Leszczynski, J., Eds.; Challenges and Advances in Computational Chemistry and Physics; Springer: Berlin, 2008; Vol.5.

(11) (a) Mennucci, B.; Toniolo, A.; Tomasi, J. *J. Am. Chem. Soc.* **2000**, *122*, 10621. (b) Mennucci, B.; Toniolo, A.; Tomasi, J. *J. Phys. Chem. A* **2001**, *105*, 7126. (c) Mennucci, B.; Toniolo, A.; Tomasi, J. *J. Phys. Chem. A* **2001**, *105*, 4749. (d) Cammi, R.; Frediani, L.; Mennucci, B.; Ruud, K. *J. Chem. Phys.* **2003**, *119*, 5818. (e) Caricato, M.; Mennucci, B.; Tomasi, J. *J. Phys. Chem. A* **2004**, *108*, 6248. (f) Mennucci, B.; Martinez, J. M. *J. Phys. Chem. B* **2005**, *109*, 9818. (g) Caricato, M.; Mennucci, B.; Tomasi, J. *Mol. Phys.* **2006**, *104*, 875. (h) Kulkarni, A. D.; Mennucci, B.; Tomasi, J. *J. Chem. Theory Comput.* **2008**, *4*, 578. (i) Mennucci, B.; Caricato, M.; Ingrosso, F.; Cappelli, C.; Cammi, R.; Tomasi, J.; Scalmani, G.; Frisch, M. J. *J. Phys. Chem. B* **2008**, *112*, 414.

(12) (a) Cammi, R.; Corni, S.; Mennucci, B.; Tomasi, J. *J. Chem. Phys.* **2005**, *122*, 104513. (b) Corni, S.; Cammi, R.; Mennucci, B.; Tomasi, J. *J. Chem. Phys.* **2005**, *123*, 134512.

(13) McWeeny, R. *Methods of Molecular Quantum Mechanics*, 2nd ed.; Academic Press: London, 1992.

(14) Foresman, J. B.; Head-Gordon, M.; Pople, J. A.; Frisch, M. J. *J. Phys. Chem.* **1992**, *96*, 135.

(15) (a) Casida, M. E. in *Recent Advances in Density Functional Methods*; Chong, D. P., Ed.; World Scientific: Singapore, 1995;.(b) Gross, E. U. K.; Dobson, J. F.; Petersilka, M. In *Density Functional Theory II*; Nalewajski, R. F., Ed.; Springer: Heidelberg, 1996.

(16) (a) Bauernschmitt, R.; Ahlrichs, R. *Chem. Phys. Lett.* **1996**, *256*, 454. (b) Stratmann, R. E.; Scuseria, G. E.; Frisch, M. J. *J. Chem. Phys.* **1998**, *109*, 8218. (c) Hirata, S.; Head-Gordon, M. *Chem. Phys. Lett.* **1999**, *314*, 291.

(17) Caricato, M.; Mennucci, B.; Tomasi, J.; Ingrosso, F.; Cammi, R.; Corni, S.; Scalmani, G. *J. Chem. Phys.* **2006**, *124*, 124520.

(18) Cammi, R.; Mennucci, B.; Tomasi, J. *J. Phys. Chem. A* **2000**, *104*, 5631.

(19) Scalmani, G.; Frisch, M. J.; Mennucci, B.; Tomasi, J.; Cammi, R.; Barone, V. *J. Chem. Phys.* **2006**, *124*, 094107.

(20) (a) Cancès, E.; Mennucci, B. *J. Math. Chem.* **1998**, *23*, 309. (b) Cancès, E.; Mennucci, B.; Tomasi, J. *J. Chem. Phys.* **1997**, *107*, 3032. (c) Mennucci, B.; Cancès, E.; Tomasi, J. *J. Phys. Chem. B* **1997**, *101*, 10506.

(21) (a) Marcus, R. A. *J. Chem. Phys.* **1956**, *24*, 966–979. (b) Brady, J. E.; Carr, P. W. *J. Phys. Chem.* **1985**, *89*, 5759. (c) Kim, H. J.; Hynes, J. T. *J. Am. Chem. Soc.* **1992**, *114*, 10508 and–10528. (d) Aguilar, M. A. *J. Phys. Chem. A* **2001**, *105*, 10393.

(22) (a) Mennucci, B.; Cammi, R.; Tomasi, J. *J. Chem. Phys.* **1998**, *109*, 2798. (b) Cammi, R.; Mennucci, B.; Ruud, K.; Frediani, L.; Mikkelsen, K. V.; Tomasi, J. *J. Chem. Phys.* **2002**, *117*, 13.

(23) Mikkelsen, K. V.; Jorgensen, P.; Jensen, H. J. A. *J. Chem. Phys.* **1994**, *100*, 6597.

(24) (a) Cammi, R.; Mennucci, B. *J. Chem. Phys.* **1999**, *110*, 9877. (b) Cammi, R.; Frediani, L.; Mennucci, B.; Ruud, K. *J. Chem. Phys.* **2003**, *119*, 5818.

(25) Cossi, M.; Barone, V. *J. Chem. Phys.* **2001**, *115*, 4708.

(26) Becke, A. D. *J. Chem. Phys.* **1993**, *98*, 5648.

(27) Handy, N. C.; Schaefer, H. F., III. *J. Chem. Phys.* **1984**, *81*, 5031.

(28) (a) Improta, R.; Barone, V.; Scalmani, G.; Frisch, M. J. *J. Chem. Phys.* **2006**, *125*, 054103. (b) Improta, R.; Scalmani, G.; Frisch, M. J.; Barone, V. *J. Chem. Phys.* **2007**, *127*, 074504.

(29) (a) Cossi, M.; Scalmani, G.; Rega, N.; Barone, V. *J. Chem. Phys.* **2002**, *117*, 43. (b) Cossi, M.; Rega, N.; Scalmani, G.; Barone, V. *J. Comput. Chem.* **2003**, *24*, 669.

(30) (a) Ingrosso, F.; Mennucci, B.; Tomasi, L. *J. Mol. Liq.* **2003**, *108*, 21. (b) Caricato, M.; Ingrosso, F.; Mennucci, B.; Tomasi, J. *J. Chem. Phys.* **2005**, *122*, 154501. (c) Mennucci, B. *Theor. Chem. Acc.* **2006**, *116*, 31.

(31) (a) Kanis, D. R.; Ratner, M. A.; Marks, T. J. *Chem. Rev.* **1994**, *94*, 195. (b) Marder, S. R.; Cheng, L. T.; Tiemann, B. G.; Friedli, A. C.; Blanchard-Desche, M.; Perry, J. W.; Skindhoj, J. *Science* **1994**, *263*, 511. (c) Bishop, D. M. *Adv. Chem. Phys.* **1998**, *104*, 1.

(32) (a) Moran, A. M.; Egolf, D. S.; Blanchard-Desce, M.; Kelley, A. M. *J. Chem. Phys.* **2002**, *116*, 2542. (b) Kelley, A. M. *Int. J. Quantum Chem.* **2005**, *104*, 602.

(33) Leng, W.; Wurthner, F.; Kelley, A. *J. Phys. Chem. A* **2005**, *109*, 1570–1575.

(34) Mennucci, B.; Cappelli, C.; Cammi, R.; Tomasi, J. *Theor. Chem. Acc.* **2007**, *117*, 1029.

(35) Guthmuller, J.; Champagne, B. *J. Chem. Phys.* **2007**, *127*, 164507.

(36) (a) Becke, A. D. *Phys. Rev. A* **1988**, *38*, 3098. (b) Lee, C. T.; Yang, W. T.; Parr, R. G. *Phys. Rev. B* **1988**, *37*, 785.

(37) (a) Tozer, D. J.; Amos, R. D.; Handy, N. C.; Roos, B. J.; Serrano-Andres, L. *Mol. Phys.* **1999**, *97*, 859. (b) Cai, Z.-L.; Sendt, K.; Reimers, J. R. *J. Chem. Phys.* **2002**, *117*, 5543. (c) Grimme, S.; Parac, M. *Chem. Phys. Chem.* **2003**, *3*, 292. (d) Dreuw, A.; Weisman, J. L.; Head-Gordon, M. *J. Chem. Phys.* **2003**, *119*, 2943.

(38) (a) Leininger, T.; Stoll, H.; Werner, H.-J.; Savin, A. *Chem. Phys. Lett.* **1997**, *275*, 151. (b) Iikura, H.; Tsuneda, T.; Yanai, T.; Hirao, K. *J. Chem. Phys.* **2001**, *115*, 3540. (c) Vydrov, O. A.; Heyd, J.; Krukau, A. V.; Scuseria, G. E. *J. Chem. Phys.* **2006**, *125*, 074106.

(39) Yanai, T.; Tew, D. P.; Handy, N. C. *Chem. Phys. Lett.* **2004**, *393*, 51.

(40) Frisch, M. J.; et al. *Gaussian Development Version*; Gaussian, Inc.; Wallingford, CT, 2008.

(41) (a) Dierksen, M.; Grimme, S. *J. Chem. Phys.* **2005**, *122*, 244101. (b) Dierksen, M. *FCFAST Ver. 1.0*; Universität Münster, Münster: Germany, 2005.

(42) Marder, S. R.; Perry, J. W.; Bourhill, G.; Gorman, C. B.; Tiemann, B. G.; Mansour, K. *Science* **1993**, *261*, 186.

(43) Nakatsuji, H. *Chem. Phys. Lett.* **1978**, *59*, 362.

(44) Peach, M. J. G.; Benfield, P.; Helgaker, T.; Tozer, D. J. *J. Chem. Phys.* **2008**, *128*, 044118.

(45) Myers, A. B. *Chem. Rev.* **1996**, *96*, 911.

(46) Besler, B. H.; Merz, K. M.; Kollman, P. A. *J. Comput. Chem.* **1990**, *11*, 431.

(47) Peticolas, W. L.; Rush, T. *J. Comput. Chem.* **1995**, *16*, 1261.

(48) (a) Lee, S.-Y.; Heller, E. J. *J. Chem. Phys.* **1979**, *71*, 4777. (b) Heller, E. J.; Sundberg, R. L.; Tannor, D. *J. Phys. Chem.* **1982**, *86*, 1822.

(49) (a) Iozzi, M. F.; Mennucci, B.; Tomasi, J.; Cammi, R. *J. Chem. Phys.* **2004**, *120*, 7029. (b) Curutchet, C.; Mennucci, B. *J. Am. Chem. Soc.* **2005**, *127*, 16733. (c) Scholes, G. D.; Curutchet, C.; Mennucci, B.; Cammi, R.; Tomasi, J. *J. Phys. Chem. B* **2007**, *111*, 6978.

(50) (a) Santoro, F.; Improta, R.; Lami, A.; Bloino, J.; Barone, V. *J. Chem. Phys.* **2007**, *126*, 084509. (b) Erratum. *J. Chem. Phys.* **2007**, *126*, 169903. (c) Improta, R.; Barone, V.; Santoro, F. *Angew. Chem., Int. Ed.* **2007**, *46*, 405.

(51) Mennucci, B.; Caricato, M.; Ingrosso, F.; Cappelli, C.; Cammi, R.; Tomasi, J.; Scalmani, G.; Frisch, M. J. *J. Phys. Chem. B* **2008**, *112*, 414.

(52) (a) Andreussi, O.; Corni, S.; Mennucci, B.; Tomasi, J. *J. Chem. Phys.* **2004**, *121*, 10190. (b) Vukovic, S.; Corni, S.; Mennucci, B. *J. Phys. Chem. C* **2009**, *113*, 121.

(53) (a) Mennucci, B. *J. Am. Chem. Soc.* **2002**, *124*, 1506. (b) Santoro, F.; Barone, V.; Gustavsson, T.; Improta, R. *J. Am. Chem. Soc.* **2006**, *128*, 16312. (c) Kongsted, J.; Mennucci, B. *J. Phys. Chem. A* **2007**, *111*, 9890. (d) Mennucci, B. Solvation models for molecular properties: continuum versus discrete approaches. In Solvation Effects on Molecules and Biomolecules: Computational Methods and Applications; Canuto, S., Ed.; Challenges and Advances in Computational Chemistry and Physics; Springer: Berlin,2008; Vol. 6.

JP8094853

Downloaded by INIST TITAN SCIENCES on September 14, 2009 | http://pubs.acs.org
Publication Date (Web): February 18, 2009 | doi: 10.1021/jp8094853